Leakage Current Elimination with Improved Non-Isolated Nine-Level Inverter for Grid-Connected PV Panels

MOHAMMAD MAALANDISH[1], SAEED POURJAFAR[2], SEYED HOSSEIN HOSSEINI[3], AND NAVID TAGHIZADEGHAN KALANTARI[4]

[1,3] *Department of Electrical and Computer Engineering, University of Tabriz, Tabriz, Iran*
[2] *Department of Electrical and Computer Engineering, University of Sahand, Tabriz, Iran*
[4] *Department of electrical engineering, azarbaijan shahid madani university, tabriz, iran.*
[*] *Corresponding author: m.maaladish.ps@gmail.com*

Manuscript received April 26, 2017; revised September 19: accepted October 09, 2017. Paper no. JEMT1704-1008

In this paper, an improved structure with model predictive control (MPC) is presented to eliminate leakage current of grid-connected PV panels. The proposed topology consists of a PV panel in the input side, a non-isolated DC/DC multilevel boost converter and a nine-level inverter at the output side. The DC-DC multilevel boost converter can provide equal voltage levels in different rated power by controlling duty-cycle. The utilized dc-dc converter can increase the output voltage of a PV panel to produce desired values at the input ports of the nine-level inverter. In Non-isolated grid-connected PV converters, there are parasitic capacitors between grid and PV panel which leads to the leakage current flowing through parasitic capacitors to the system. It causes a safety problem, injection of harmonic current to the grid, increasing losses, and efficiency reduction. In order to eliminate leakage current due to use of the parasitic capacitor of PV panel, MPC control method is utilized to achieve high overall efficiency. To confirm the operation of presented structure and theoretical analysis, PSCAD/EMTDC software is used.

keywords: *Grid-connected, Non-Isolated Converter, Multi-Level Inverter, Leakage Current, Model Predictive Controller.*

http://dx.doi.org/10.22109/jemt.2017.83238.1008

1. INTRODUCTION

Nowadays the photovoltaic power systems are one of the popular sources in renewable energy field. PV panel is one of the most efficient techniques for getting the green energy to solve environmental problems caused by fossil fuels. Distributed grid connected PV panels are playing an increasing role as an integral part of the electrical grid [1, 2]. Based on the newest report on installed PV power, the milestone of 100GW PV system was achieved at the end of 2012, and the majority were grid-connected [3, 4].

There are some challenges in PV systems as follows [5]:

- The value of generated voltage by PV panels is low and is changed by ambient temperature and solar radiation.
- Harmonic distortion of injected current should be low.
- The capability of the used converter to track maximum power point.
- Reduction of leakage current of PV panels' parasitic capacitors.
- Increasing the efficiency of PV panel.

Grid-connected PV systems often comprise a transformer, which can make isolation between grid and PV panel leads to enhance protection [5]. The most important multilevel converter topology is full-bridge converter which requires the least number of power electronic components. However, the voltage across parasitic capacitors of full-bridge converter consists of voltage ripple with high frequency which leads to the following leakage current substantially. In safety standard, the value of leakage current should be lower than 300mA. To satisfy this standard, some structures have been proposed which can provide a constant voltage across the parasitic capacitor and minimize the leakage current [6]. Grid-connected inverters comprise with embedded transformer and non-embedded transformer. To isolate PV panel from the grid and adjust the input DC voltage of the inverter, embedded transformer topologies often used.

However, the transformer is large in size and weight which lead additional losses and make the system complex. The transformerless topology has low cost, and light weight and size. One of the important issues in the transformerless grid-connected PV applications is galvanic connection of the grid and PV system that leads to leakage current problems [5–9]. However, there are some drawbacks in terms of transformerless inverters. Transformerless inverter causes the direct connection of PV panel with the grid. The high-frequency switching of the power devices leads to the existence of high-frequency common-mode voltage. Then the high-frequency leadw to the common-mode current flows between the inverter, parasitic capacitance of PV panel and grid. These factors could lead the leakage current of the common-mode circuit. Leakage current is the current that flows from conductive or surface of non-conductive parts to ground. The leakage current with high-frequency will produce the interference of conduction and radiation, which increase the harmonics of grid current and losses, and put the staffs in danger. Leakage current mitigation can be addressed by several methods such as MPC control method [10–12].

Due to the European standard VDE0126-1-1 leakage current should not exceed 300mA. To confirm this standard, many topologies have been presented such as half-bridge topology, and bipolar SPWM full bridge topology which can ensure constant voltage through the parasitic capacitors and also minimize the leakage current. In single-phase full-bridge transformerless PV inverters common-mode voltageshould be constant without high-frequency changes. Some solutions are implemented to suspend the common-mode leakage current. These solutions divided into two parts: DC-based and AC-based decoupling configurations. The DC-based decoupling configurations are performed by incorporating a DC decoupling network on the DC side. It provides the decoupled freewheeling path, such as H5, H6, optimized H6, and active clamped H6 transformerless inverters [13–16]. These inverters have three or four power switches in the conduction path, which will reduce the conversion efficiency. Meanwhile, the AC decoupling inverters have an AC decoupling circuit between the full-bridge module and output filter inductors to provide a decoupled freewheeling path. The half-bridge topology needs twice of the input voltage that is required by the full-bridge topology and generally necessitates the use of either a large PV string or a previous boost dc–dc stage. Full bridge with bipolar SPWM generates no variable common-mode voltages [17,18]. However, bipolar SPWM causes a large current ripple and high switching losses and decreases the overall efficiency of the inverter [19]. To control the current of grid-connected multilevel inverters many topologies have been investigated. One of this method that has been used in [20,21] is hysteresis current control to generate switching signals. However, this controller with respect to frequency is not optimized. In this paper an improved topology consisting of three back to the back switch, a dc-dc multilevel converter, and a nine-level inverter. The presented dc-dc converter can maintain equal output voltages by controlling duty-cycle. The proposed structure has advantages as follows:

- Continuous input current
- High voltage gain with lower duty-cycle
- Same output and multilevel with one input PV panel
- Reduction of leakage current
- High efficiency

Theoretical analysis are presented in section 2 and control method is discussed in the third section. Simulation results are finally presented to show the excellent performance of the proposed topology.

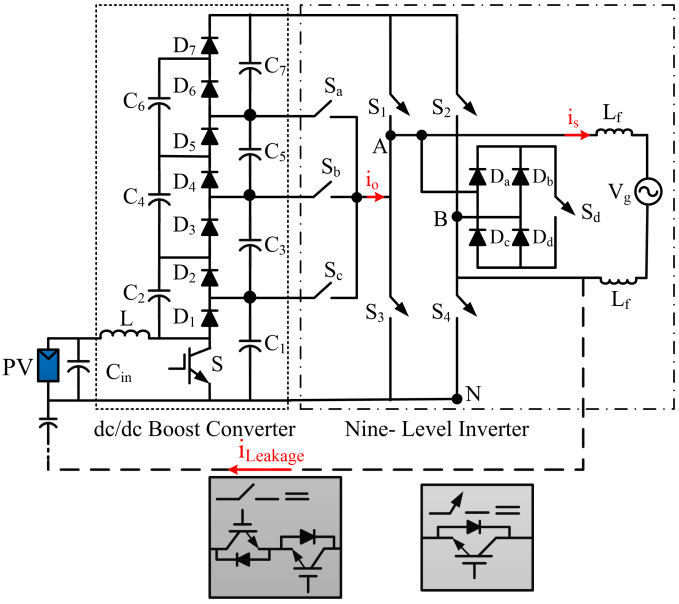

Fig. 1. The presented multilevel structure

2. PROPOSED STRUCTURE AND PRINCIPLE OF OPERATION

A. Proposed Structure

Overall PV systems comprise a PV panel and an interfacing converter such as a multilevel dc-dc converter and also a multilevel inverter. The dc-dc converter can track maximum power point. According to Fig. 1, the presented hybrid structure in this paper consists of the first three blocks which are implemented to produce multilevel inverter. Fig. 1, indicates the hybrid structure. The topology is composed of the following three parts:

- PV power supply
- Multilevel dc-dc converter with similar voltage
- Full-bridge nine level inverter

B. Multi level dc-dc converter

Fig. 2 shows the multilevel dc-dc converter which has been proposed in [22]. The difference between conventional boost converters with the proposed topology is a multilevel output voltage and also a power level production. In other words, the output voltage is four times a capacitor voltage.

The circuit of the conventional boost converter is shown in Fig. 2. When the power switch is on-state, the inductor receives the energy by input source. If the capacitor voltage C1 (VC1) is greater than the capacitor voltage C2 (VC2), VC1 clamps VC2 through the power switch (S) and D2. If the sum of the voltage of the capacitor C1 and C3 (VC1+VC3) is greater than the sum of the voltage of the capacitor C2 and C4 (VC2+VC4), VC1+VC3 clamps VC2+VC4 through S and D4. In a similar way, if VC1+ VC3+VC5 is greater than VC2+VC4+VC6, VC1+VC3+VC5 clamps VC2+ VC4+VC6 through S and D6. When the power switch is off-state, we have:

If the diode D1 is forward-bias, the capacitor C1 will charge. When the diode D3 is forward-bias, the voltage of Vin-VL+VC2 clamps C1 and C3 through the diode D3. In a similar way, when the diodes D5 and D7 is forward-bias, can be said as follows: Vin-VL+VC2+VC4 clamps C1, C3 and C5 through the diode D3

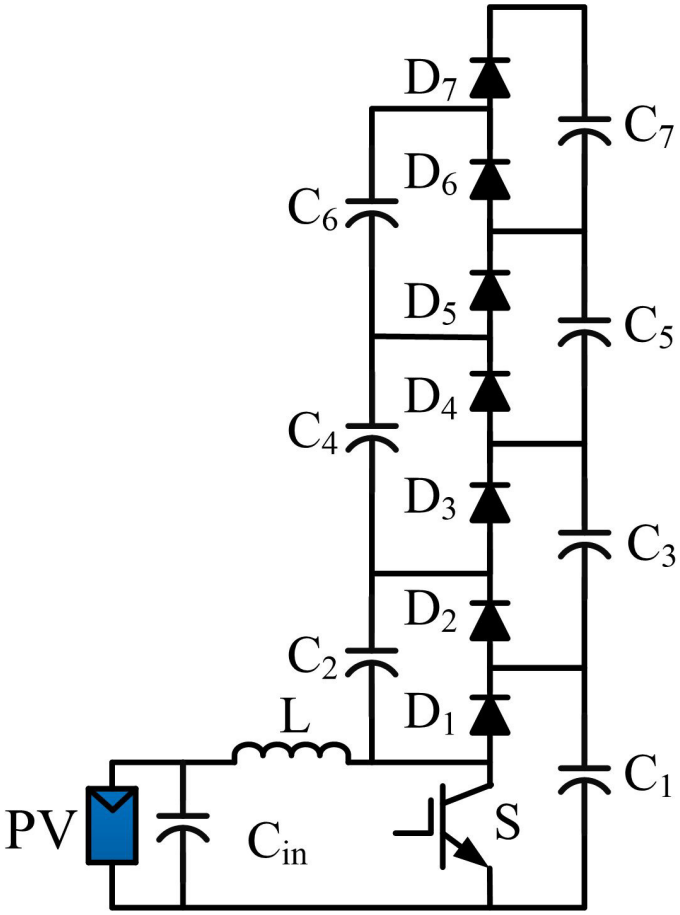

Fig. 2. Multilevel dc-dc converter presented in [22]

and Vin-VL+VC2+VC4+ VC6 clamps C1, C3, C5 and C7 through the diode D5.

Therefore, by applying the voltage balancing law on inductor L (the voltage average of each inductor in one period is zero), the voltage gain of the dc-dc converter is four-time of the conventional boost converter and obtained as follows:

$$\frac{V_o}{V_{in}} = \frac{4}{1-D} \tag{1}$$

The operation of this converter consists of 8 modes in one switching period that is discussed in [22].

C. Nine-Level Inverter

The proposed nine level inverter in this paper is an improved structure that is presented in [23]. As shown in Fig.3, this topology comprises a full bridge inverter. The inverter consists of three back to back switch and four capacitors as a dc link voltage divider. The performance of the switches in the circuit is that in addition to producing half level dc link voltage, it can reduce the layout complexity comparatively with floating capacitors, diode clamp topology and hybrid structure that is mentioned in [24,25]. The proposed nine level inverter is shown in Fig. 3, has an advantage of few number of power switches, power diodes, and capacitor in comparison with the inverters with similar voltage level. The nine-level converter can produce nine-voltage level $(+V_d + \frac{3}{4}V_d + \frac{1}{2}V_d + \frac{1}{4}V_d - \frac{1}{4}V_d - \frac{1}{2}V_d - \frac{3}{4}V_d - V_d)$ from the

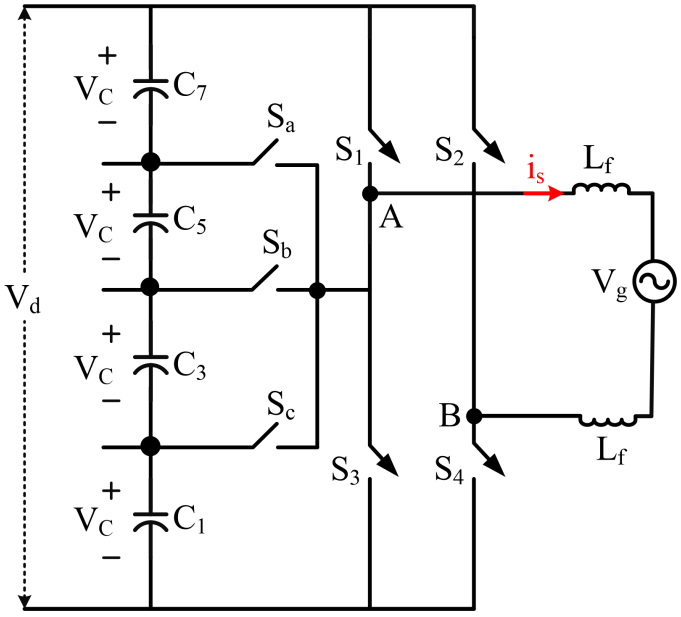

Fig. 3. Nine level inverter

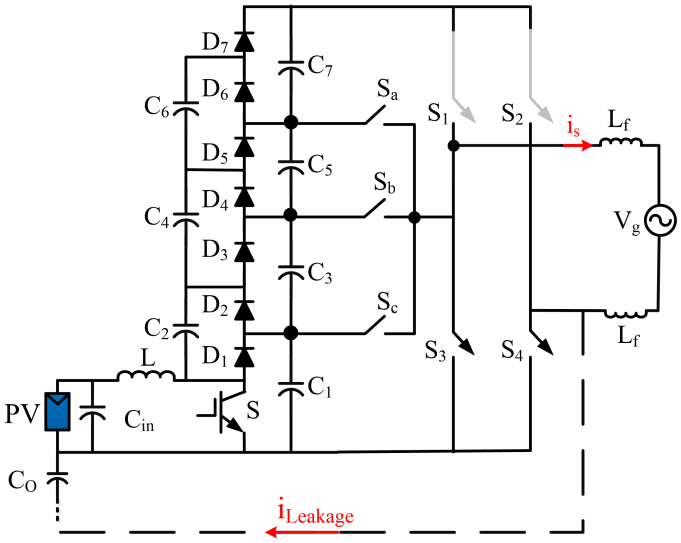

Fig. 4. Leakage current in nine level inverter when S_3 and S_5 turn ON

dc-link power supply. The switching state of this topology to generate different voltage level is indicated in Table 1.

In isolated topologies leakage current path has been cut off by transformer so the leakage current is very low. Grid-connected non-isolated transformerless inverters have the advantage of low cost, small size, light weight and high efficiency. However, one drawback of these systems with PV power supply is leakage current [5]. As shown in Fig. 4 when S_3 and S_4 are turned ON, the leakage current flows through the parasitic capacitor of the panel, filter (L_f), full bridge and grid. Thus in transformerless structure, undesirable leakage current leads to produce electromagnetic interference (EMI). So the value of leakage current should be lower than 300mA [26].

To eliminate leakage current, the voltage across the parasitic capacitor of PV panel should be constant. In other words, to produce zero level S_3 and S_4 should not turn on simultaneously. In

Table 1. SWITCHING STATES OF NINE-LEVEL CONVERTER

Switch	S_a	S_b	S_c	S_1	S_2	S_3	S_4
$+V_d$	0	0	0	1	0	0	1
$+\frac{3}{4}V_d$	1	0	0	0	0	0	1
$+\frac{1}{2}V_d$	0	1	0	0	0	0	1
$+\frac{1}{4}V_d$	0	0	1	0	0	0	1
0	0	0	1	0	0	0	1
0	0	0	1	0	0	0	1
$-\frac{1}{4}V_d$	1	0	1	0	0	1	0
$-\frac{1}{2}V_d$	0	1	0	0	0	1	0
$-\frac{3}{4}V_d$	0	0	1	0	0	1	0
$-V_d$	0	0	0	0	1	1	0

this case, the leakage current of PV panel may lead to reducing overall system efficiency and also reduce panel lifetime. Thus, when the zero level operates, the new freewheeling path would have existed to isolate the panel from grid. It leads to eliminate leakage current. Various solutions have been developed to eliminate leakage current. In this paper an enhanced topology with one power switch and four diodes are utilized.

D. Leakage current elimination

In 2006, Sunway manufacturer patented a new structure with common FB inverter. This topology became known as a HERIC. It was created by adding a bypass leg using two back to back switch in ac part of the common FB inverter. Nine-level inverter with four-diode and one power switch is shown in Fig. 6. This topology's operation is similar to HERIC structure. The only difference is that one switch eliminate and two diodes added.

As shown in Fig. 5, the operation of proposed multilevel inverter can divide into nine switching states. Table 2 indicates the different state of the nine-level inverter with four-diode and one power switch. The switching state of this topology with four-diode and one power switch at output voltage is provided in Table 2.

For eliminating the leakage current, the voltage of common mode must be constant in each period. Table 3 illustrates that the voltage of common mode is constant in each period. Therefore, the voltage of common mode in one period as shown in Table 2:

Based on Table 1 and Table 2, it is clear that by contrast Fig.6 structure to provide zero voltage level, S_3 and S_4 should turn-on at the same time. As shown in Fig. 6, in zero voltage level S_a, D_a and D_d are turned on or S_d, D_b and D_C are turned on. It can lead to isolated PV panel from the grid, so it causes to reduce leakage current. Fig.6 (a and b) indicates that the is turned on and leakage current has been eliminated.

Therefore bypass leg comprises one power switch and four diodes. It has some advantages as follows:

- It prevents reactive power exchange between inductive fil-

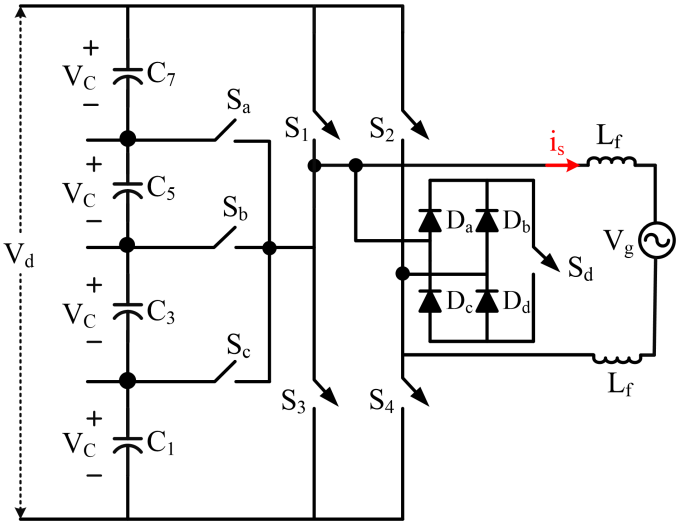

Fig. 5. Nine level inverter with leakage current elimination

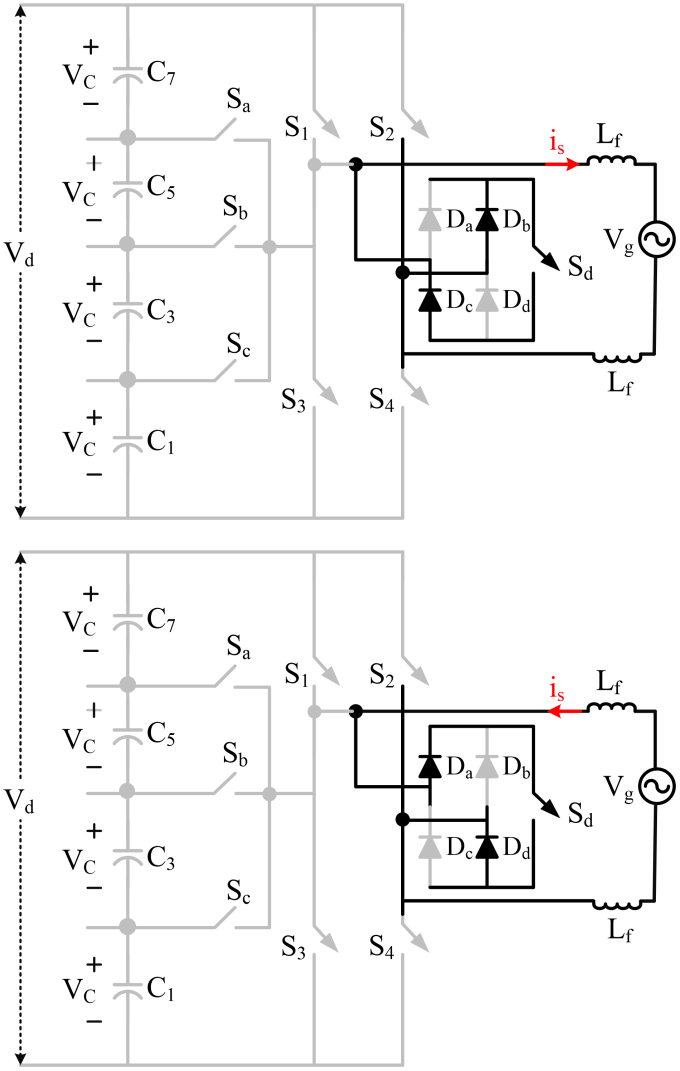

Fig. 6. Current paths in the nine level inverter.

Table 2. SWITCHING STATES OF NINE-LEVEL CONVERTER

state	S_1	S_2	S_3	S_4	S_a	S_b	S_c	S_d	D_a	D_b	D_c	D_d	V_{AN}	V_{BN}	V_{AB}	$V_{AN}-V_{BN}$
1	1	0	0	1	0	0	0	0	0	0	0	0	V_d	0	V_d	V_d
2	0	0	0	1	1	0	0	0	0	0	0	0	$0.75V_d$	0	$0.75V_d$	$0.75V_d$
3	0	0	0	1	0	1	0	0	0	0	0	0	$0.5V_d$	0	$0.5V_d$	$0.5V_d$
4	0	0	0	1	0	0	1	0	0	0	0	0	$0.25V_d$	0	$0.25V_d$	$0.25V_d$
5	0	0	0	0	0	0	0	1	0	1	1	0	0	0	0	0
6	0	0	0	0	0	0	0	1	1	0	0	1	0	0	0	0
7	0	1	0	0	1	0	0	0	0	0	0	0	$0.75V_d$	V_d	$-0.25V_d$	$-0.25V_d$
8	0	1	0	0	0	1	0	0	0	0	0	0	$0.5V_d$	V_d	$-0.5V_d$	$-0.5V_d$
9	0	1	0	0	0	0	1	0	0	0	0	0	$0.25V_d$	V_d	$-0.75V_d$	$-0.75V_d$
10	0	1	1	0	0	0	0	0	0	0	0	0	0	V_d	$-V_d$	$-V_d$

ters ($L_{f1(2)}$) and input capacitors (C_{in}) in zero level which increases the efficiency.

- In zero level switching, isolate PV from grid and minimize leakage current
- Reduce Harmonic distortion of injected current

3. MODEL PREDICTIVE CONTROL

Model predictive control for power converters and drives is a control technique that has been considered in the research community for the last years. The main reason is that MPC presents high computational burden. It can solve the conventional control method issues, such as nonlinear system limitations, multivariate systems and quality of systems. This is important to have an appropriate mathematical models to predict the behavior of variables under control for electrical and mechanical systems in MPC method. Moreover, it can be a large amount of computation required to perform high-speed and low-cost.

Model Predictive Control (MPC) is a controller method which uses the model of the system to predict the future behavior of the controlled variables by considering a prediction horizon N. For MPC, the used algorithm is executed again every sampling period and only the first magnitude of the optimal sequence is used to the studied system at instant k [27]. In general, the most usual cost function of MPC is:

$$g = \sum_i \lambda_i (X_i^* - X_i^p)^2 \tag{2}$$

where X_i^* and X_i^p represent the reference command and the predicted magnitude of a variable X_i , respectively. In fact, for every switching state of the converter, MPC predicts (using the mathematical model) the behavior of variable Xin the next sampling interval X^p. Also, λ_f is the weighting factor and g is the cost function and the index I is the number of controlled variables.

A. Principle of Operation MPC

Fig. 8, indicates a block diagram of MPC. It used a method for forecasting future periods based on the value of the current and future output composed with future control. In fact, this process defines as follows [27]:

1. Measure the controlled variables
2. Apply the optimal switching states which have been calculated in previous sampling period.
3. For each switching state of the converter, predict the behavior of variable X using the mathematical model at next sampling period.

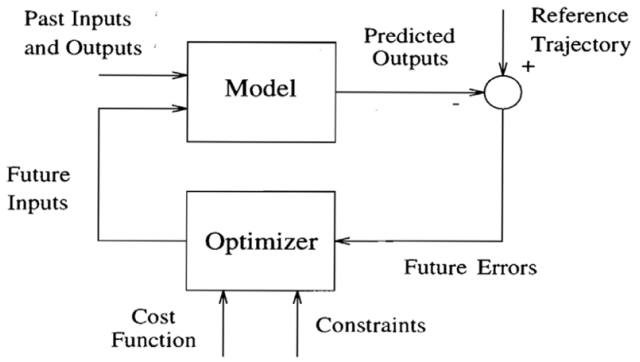

Fig. 7. MPC block diagram

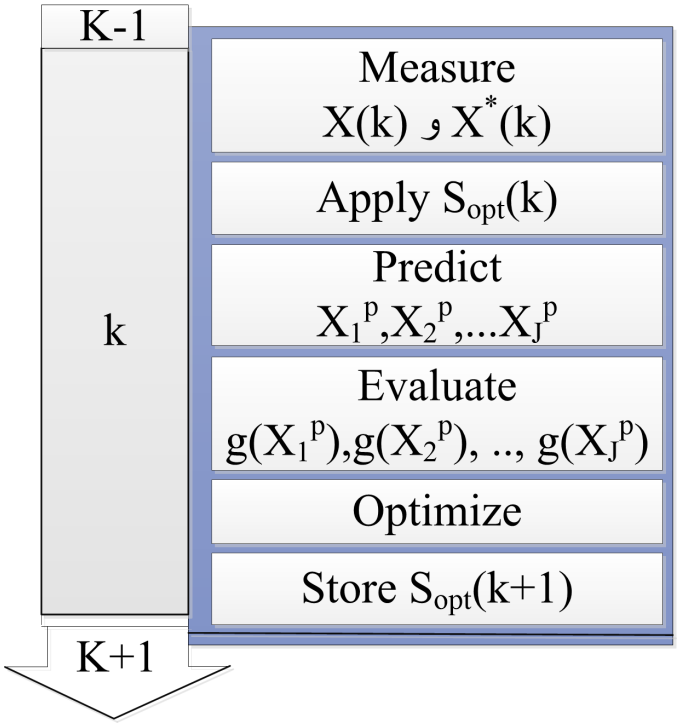

Fig. 8. Time diagram of the execution of the MPC algorithm

4. Evaluate the cost function or error for each prediction as follows:

$$g = |X^* - X^p| \tag{3}$$

5. Select the switching state (S_{opt}) that minimize the cost function and store it for use at the next sampling period.

B. Nine Level Inverter with MPC Analysis

We consider f and f_s as grid and switching frequencies, respectively. Since ($f_s >> f$) we can suppose that grid voltage (V_g) is constant in one switching period. To calculate MPC method by applying KVL for the circuit as shown in Fig. 9, we have:

$$2L_f \frac{di_s}{dt} + R_f i_s + V_g = V_{AB} \tag{4}$$

$$2L_f \frac{\Delta i_s}{\Delta t} + R_f i_s + V_g = V_{AB} \tag{5}$$

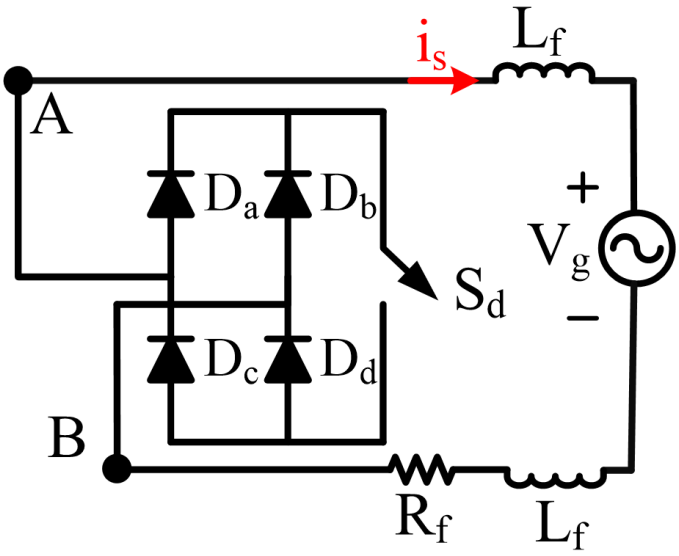

Fig. 9. Nine level inverter for MPC analysis

In (5) and are filtering element and is grid current. (5) can be rewritten for a switching period by using MPC method as follows:

$$2L_s\frac{i_s(k+1)-i_s(k)}{T}+R_f i_s(k)+V_g(k)=V_{AB}(k) \quad (6)$$

i_s, V_g and

$indicatedwithsensors.Withthecombinationof(5)and(6),wehave:$

$$i_s(k+1)=\frac{T_s}{2L_f}(V_{AB}(k)-V_g(k))-\frac{R_f}{2L_f}T_s i_s(k)+i_s(k) \quad (7)$$

By knowing V_g and i_s at time k, the grid current can be estimated at $k+1$. MPC method predicts the behavior of grid current for any generated voltage levels by nine-level inverter through (V_{AB}). In fact, based on the presence of different voltages vector, performs a specific function. The magnitudes of V_{AB} are as same as the nine-level voltages according to Table 2. Thus, for the number of voltage levels, there will be a number of current prediction. If the reference grid current is a sinusoidal current according to (8):

$$i_{s-ref}=I_{m-ref}sin\omega t \quad (8)$$

$$e_j=(i_s(k+1)|_{V_{AB}=jV_d}-i_{s-ref}(k+1))^2 \quad (9)$$

By using MPC method, it can be mentioned that at time k, the switching vector is selected as switching vectors which mean that the cost function or the error related to its vector should be minimum in comparison with other switching vectors. In fact, appropriate switching vector for any time has chosen by last seconds.

In photovoltaics systems connected to the grid, not only the load current harmonics and reactive power compensation should be provided, but also it must inject the active power to the grid. in this study, the current and voltage are the same phase at the grid section by MPC control method, hence the reactive power compensation does not happen.

C. The Efficiency Calculation

The efficiency of the dc-dc converter can be calculated as follows:

$$\begin{cases}\eta_{DC-DC(converter)}=\frac{P_o}{P_o+\Delta P}\times 100\% \\ \Delta P=A_1+A_2+A_3+A_4+A_5+A_6 \\ =(A_1=r_{DS-ON}\times {I_{av_{on}}}^2)+(A_2=\left[\frac{1}{2}C_S(\frac{V_i}{1-D})^2 f_S\right]) \\ +(A_3=r_L {I_{av_L}}^2)+ \\ (A_4=\sum_{m=1}^{7}(r_{F_{Dm}}\times {I_{av_m}}^2))+(A_5=\sum_{m=1}^{7}(V_{F_{Dm}}\times I_{av_m}))+ \\ (A_6=\sum_{m=1}^{7}(r_{R_{C_m}}\times {I_{R_{C_m}}}^2))\end{cases} \quad (10)$$

where,

A_1: The power losses of the switches, A_2: The switching losses, A_3: The conduction losses of inductors, A_4: The diode voltage drop losses, A_5: The diodes forward voltage losses, A_6: The power losses of capacitors.

The whole efficiency of the system can be obtained as follows:

$$\eta_{system}\%=\eta_{DC-DC(converter)}\times\eta_{inverter}\times 100\% \quad (11)$$

4. COMPARISON STUDY

By observing the Table 3, it is clear that the proposed structure has less leakage current among other structures. The leakage current of the proposed structure is about 0.72%. In addition, the THD of the proposed structure is 4.38% and can be said this value is suitable for each inverter that it will be connected to the grid.

5. SIMULATION RESULTS

The proposed structure is simulated using PSCAD/EMTDC software. A PV panel with maximum rated voltage and current of 74V and 32A is used in the simulation. The characteristic of PV panel and the proposed converter is shown in Table 4. Fig. 10 illustrates the circuit schematic of the proposed converter and the control of switches with MPC control method in PSCAD/EMTDC comprehensive. Simulation results for MPC method are indicated in Figs. 11 - 15. Based on Fig. 11, It is clear that because of nine level inverter in output, the injected current is almost sinusoidal current with small ripple and also able to track the reference current. Furthermore, from Fig. 12 it is obvious that both grid voltage and injected current are in phase. It means that the power factor is unity. The nine-level output voltage is shown in Fig. 5. It shows that this voltage is a completely symmetrical and floating between +380 to -380. Dc-link voltage is illustrated in Fig. 13. When PV panel operates in maximum power point, dc-link voltage with low current ripple can be regulated in 380v and it is four-time of the output voltage of dc-dc converter capacity. It leads to being transferred Maximum power from nine-level inverter to grid. Fig. 14 indicates the leakage current using the proposed structure. Based on the Fig. 14 the amplitude of the leakage current is 7mA. Fig. 15 illustrate THD of injected current. Based on Fig. 15, the value of injected current is about 4.38%. It is clear that by using this structure, the voltage through the parasitic capacitor (C_0) is constant and also it causes to reduce the effective value of leakage current.

Table 3. COMPARISON BETWEEN THE PROPOSED STRUCTURE AND OTHER STRUCTURES

Converter Topology	[8]	[9]	[10]	[21]	[27]	Proposed
Capacitor Voltage Balancing	symmetric	symmetric	symmetric	symmetric	symmetric	symmetric
Switch no.	8	10	8	7	6	5
Leakage current	5mA	7.7mA	5.4mA	8mA	6mA	7mA
Efficiency %	97.4	97	94.6	94.4	95	92.93
THD %	2.4	3.5	4.98	3.6	13	4.38
Power level	500W	2kW	1kW	600W	-	2.35kW

Table 4. THE CHARACTERISTIC OF PV PANEL AND PROPOSED CONVERTER

	Parameter	Value
PV	Open circuit voltage (V_{OC}	90 V
	Short circuit current (I_{SC}	62 A
	The parasitic resistance (R_o)	1Ω
	Parasitic capacitors (C_o)	0.1 μF
Converters	input voltage (V_{in})	74 V
	DC link voltage (V_{dc})	180 V
	Switching frequency (f_s)	5 kHz
	Voltage network / Frequency	$220^{Vrms}/50^{Hz}$
	Input inductance (L)	1mH
	Equivalent series resistance (R_c)	5mΩ
	Output capacitance	2200 μF
	Output inductance	2.5mH

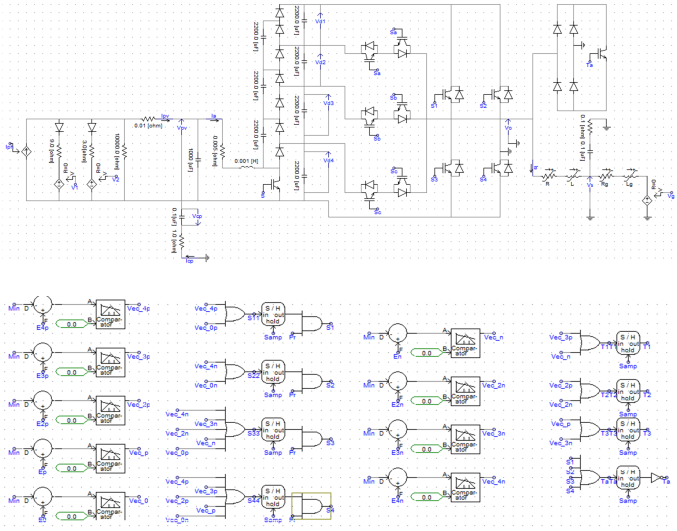

Fig. 10. (a) The circuit schematic of the proposed structure in PSCAD/EMTDC comprehensive, (b) The control of switches with MPC control method.

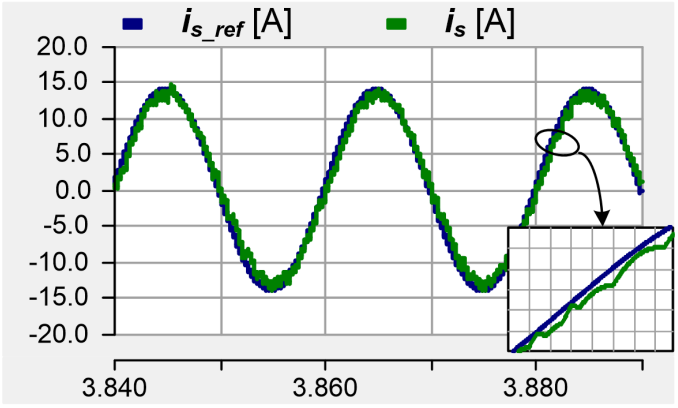

Fig. 11. Grid and reference current waveforms comparison

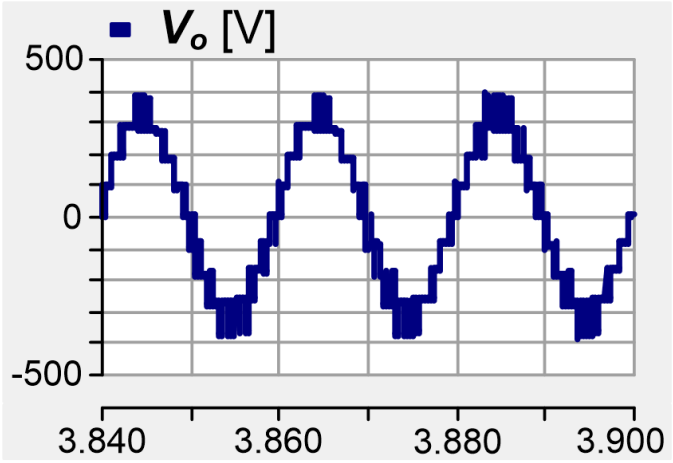

Fig. 16 illustrates the output current and output voltage of the PV panel which is connected to input side structure. With regarding Fig. 16, it is evident that the output voltage of PV panel is low for connected to the grid, so by using a DC-DC

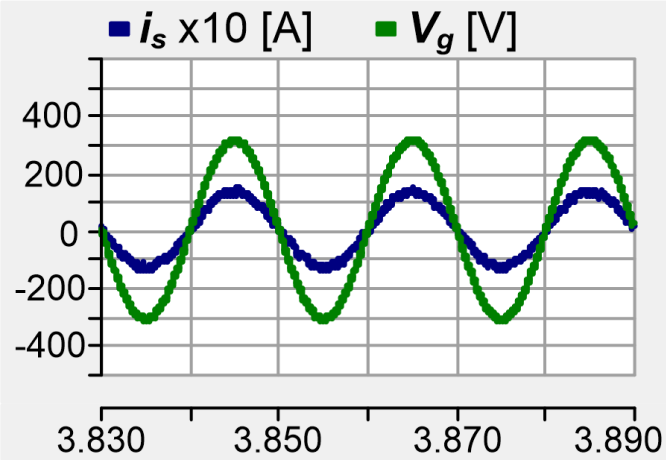

Fig. 12. Grid voltage and injected current are in phase

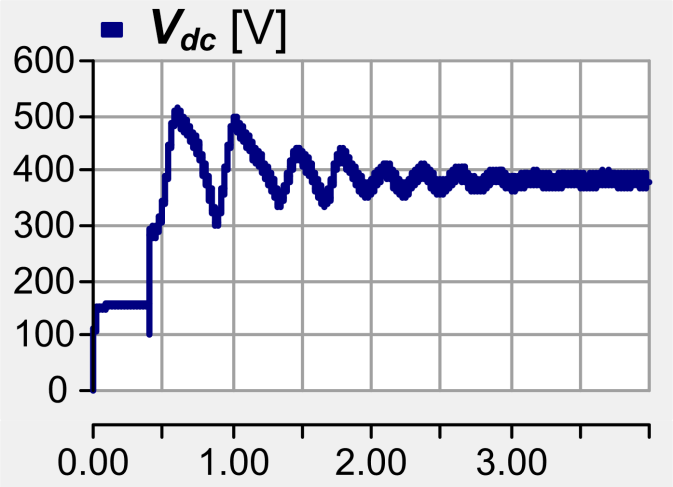

Fig. 13. DC-link voltage

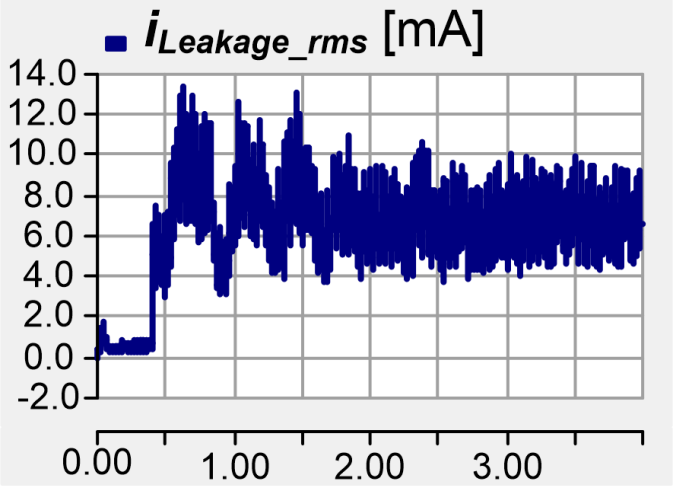

Fig. 14. Leakage current with proposed stricter in input

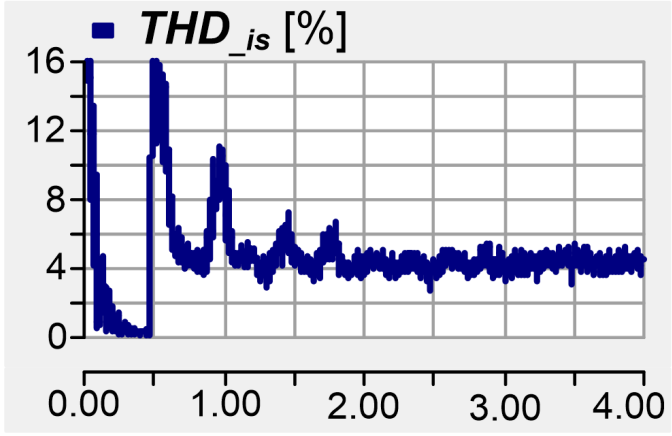

Fig. 15. THD waveform of injected current

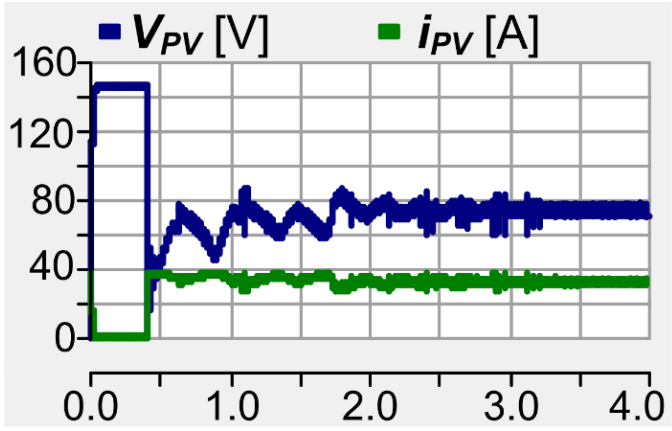

Fig. 16. The output current and output voltage of the PV panel.

converter can be achieved high voltage level for connected the grid. Based on Fig. 17, it is clear that the input current of DC-DC converter similar to the output current of PV panel, just the difference is that the current ripple of the PV panel is higher than the current ripple of DC-DC converter. Fig. 18 illustrates the output power of the PV panel which is about 2.35 kW. Fig. 12(d) illustrates the output power of PV panel versus the output voltage of PV panel. Based on this Fig. 19, it can be seen that the maximum value of the output power is achieved when the output voltage of PV panel is about 74 V. By comparing Figs. 16 and 18, it is clear that the maximum power of PV panel is achieved when the output voltage is about 74 V. According to these explanations, the DC-DC converter is able to achieve the MPPT (maximum power point tracking).

6. CONCLUSION

In this paper, an improved new combinatorial topology has been presented for grid-connected PV application. The proposed structure comprises a multilevel dc-dc boost converter for raising PV panel voltage level. Also, dc-dc multi-output converter presented to produce equal voltage. It makes the structure appropriate for photovoltaic systems. Furthermore, an inverter with approximately sinusoidal output has been utilized which provide nine level output voltage. In addition, it leads to the current flow from the power supply to the grid and thus, produce

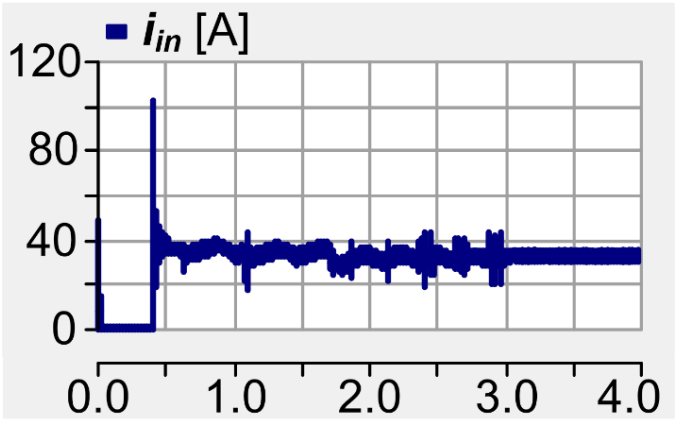

Fig. 17. The input current of the DC-DC converter

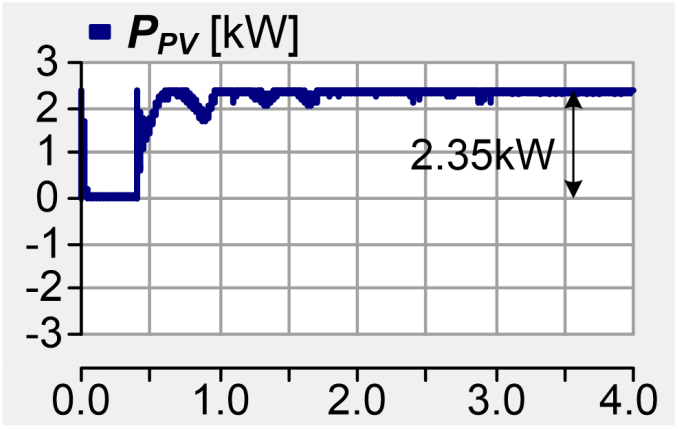

Fig. 18. The output power of the PV panel

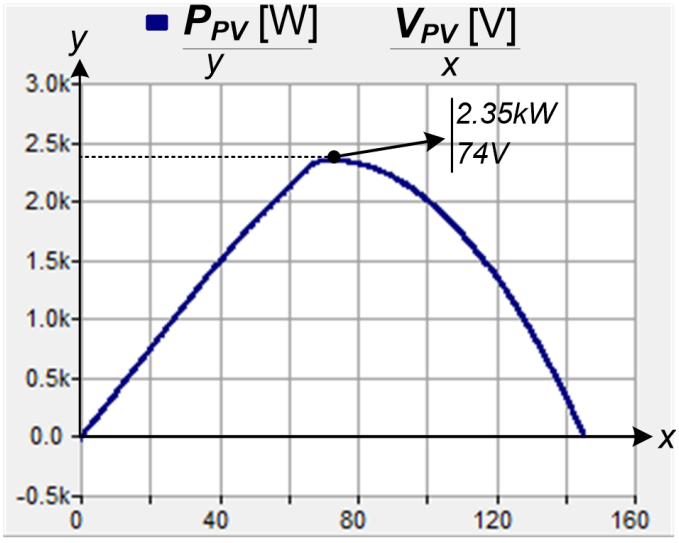

Fig. 19. the output power of PV panel versus the output voltage of PV panel.

a good power quality. Moreover, injected current controlled by MPC method to select appropriate switching vectors for the inverter. In fact, MPC method control used to achieve lower leakage current, lower THD, and higher efficiency about 92.93%. Also, reducing the effects of EMI on instrumentation signals.

REFERENCES

1. J. F. Ardashir, M. Sabahi, S. H. Hosseini, F. Blaabjerg, E. Babaei, and G. B. Gharehpetian, "A single-phase transformerless inverter with charge pump circuit concept for grid-tied pv applications," *IEEE Transactions on Industrial Electronics*, vol. 64, no. 7, pp. 5403–5415, 2017.

2. A. A. Saeidabadi and S. H. Hosseini, "A novel transformerless photovoltaic grid-connected current source inverter with ground leakage current elimination," *2017 8th power electronics, drive systems technologies conference (PEDSTC),Mashhad*, pp. 61–66, 2017.

3. H. D. Paulino, P. J. M. Menegáz, and D. S. L. Simonetti, "A review of the main inverter topologies applied on the integration of renewable energy resources to the grid," in *Power Electronics Conference (COBEP), 2011 Brazilian*, pp. 963–969, IEEE, 2011.

4. B. Guha, R. J. Haddad, and Y. Kalaani, "Voltage ripple-based passive islanding detection technique for grid-connected photovoltaic inverters," *IEEE Power and Energy Technology Systems Journal*, vol. 3, no. 4, pp. 143–154, 2016.

5. M. Islam, S. Mekhilef, and F. M. Albatsh, "An improved transformerless grid connected photovoltaic inverter with common mode leakage current elimination," 2014.

6. W. Cui, H. Luo, Y. Gu, W. Li, B. Yang, and X. He, "Hybrid-bridge transformerless photovoltaic grid-connected inverter," *IET Power Electronics*, vol. 8, no. 3, pp. 439–446, 2015.

7. S. B. Kjaer, J. K. Pedersen, and F. Blaabjerg, "A review of single-phase grid-connected inverters for photovoltaic modules," *IEEE transactions on industry applications*, vol. 41, no. 5, pp. 1292–1306, 2005.

8. M. Sabahi, S. H. Hosseini, F. Blaabjerg, E. Babaei, G. B. Gharehpetian, *et al.*, "Transformerless inverter with charge pump circuit concept for pv application," *IEEE Journal of Emerging and Selected Topics in Power Electronics*, 2016.

9. S. A. Khan, Y. Guo, and J. Zhu, "A high efficiency transformerless pv grid-connected inverter with leakage current suppression," in *Electrical and Computer Engineering (ICECE), 2016 9th International Conference on*, pp. 190–193, IEEE, 2016.

10. C. A. Rojas, M. Aguirre, S. Kouro, T. Geyer, and E. Gutierrez, "Leakage current mitigation in photovoltaic string inverter using predictive control with fixed average switching frequency," *IEEE Transactions on Industrial Electronics*, 2017.

11. H. Xiao, S. Xie, Y. Chen, and R. Huang, "An optimized transformerless photovoltaic grid-connected inverter," *IEEE Transactions on Industrial Electronics*, vol. 58, no. 5, pp. 1887–1895, 2011.

12. L. Zhang, K. Sun, L. Feng, H. Wu, and Y. Xing, "A family of neutral point clamped full-bridge topologies for transformerless photovoltaic grid-tied inverters," *IEEE Transactions on Power Electronics*, vol. 28, no. 2, pp. 730–739, 2013.

13. L. Wang, Y. Shi, Y. Shi, R. Xie, and H. Li, "Ground leakage current analysis and suppression in a 60 kw 5-level t-type transformerless sic pv inverter," *IEEE Transactions on Power Electronics*, 2017.

14. B. Yang, W. Li, Y. Gu, W. Cui, and X. He, "Improved transformerless inverter with common-mode leakage current elimination for a photovoltaic grid-connected power system," *IEEE Transactions on Power Electronics*, vol. 27, no. 2, pp. 752–762, 2012.

15. H. Xiao, S. Xie, Y. Chen, and R. Huang, "An optimized transformerless photovoltaic grid-connected inverter," *IEEE Transactions on Industrial Electronics*, vol. 58, no. 5, pp. 1887–1895, 2011.

16. G. San, H. Qi, J. Wu, and X. Guo, "A new three-level six-switch topology for transformerless photovoltaic systems," in *Power Electronics and Motion Control Conference (IPEMC), 2012 7th International*, vol. 1, pp. 163–166, IEEE, 2012.

17. J. M. Myrzik and M. Calais, "String and module integrated inverters for single-phase grid connected photovoltaic systems-a review," in *Power Tech Conference Proceedings, 2003 IEEE Bologna*, vol. 2, pp. 8–pp, IEEE, 2003.

18. R. González, J. Lopez, P. Sanchis, and L. Marroyo, "Transformerless inverter for single-phase photovoltaic systems," *IEEE Transactions on Power Electronics*, vol. 22, no. 2, pp. 693–697, 2007.

19. R. González, E. Gubía, J. López, and L. Marroyo, "Transformerless single-phase multilevel-based photovoltaic inverter," *IEEE Transactions on Industrial Electronics*, vol. 55, no. 7, pp. 2694–2702, 2008.

20. A. K. Panda and Y. Suresh, "Research on cascade multilevel inverter with single dc source by using three-phase transformers," *International Journal of Electrical Power & Energy Systems*, vol. 40, no. 1, pp. 9–20, 2012.

21. Y. Hu, W. Cao, B. Ji, J. Si, and X. Chen, "New multi-stage dc–dc converters for grid-connected photovoltaic systems," *Renewable Energy*, vol. 74, pp. 247–254, 2015.

22. J. C. Rosas-Caro, J. M. Ramirez, F. Z. Peng, and A. Valderrabano, "A dc–dc multilevel boost converter," *IET Power Electronics*, vol. 3, no. 1, pp. 129–137, 2010.

23. N. A. Rahim, K. Chaniago, and J. Selvaraj, "Single-phase seven-level grid-connected inverter for photovoltaic system," *IEEE transactions on industrial electronics*, vol. 58, no. 6, pp. 2435–2443, 2011.

24. A. K. Panda and Y. Suresh, "Research on cascade multilevel inverter with single dc source by using three-phase transformers," *International Journal of Electrical Power & Energy Systems*, vol. 40, no. 1, pp. 9–20, 2012.

25. B. Singh, N. Mittal, K. Verma, D. Singh, S. Singh, R. Dixit, M. Singh, and A. Baranwal, "Multilevel inverter: A literature survey on topologies and control strategies," *International Journal of Reviews in Computing*, vol. 10, 2012.

26. L. Zhang, K. Sun, L. Feng, H. Wu, and Y. Xing, "A family of neutral point clamped full-bridge topologies for transformerless photovoltaic grid-tied inverters," *IEEE Transactions on Power Electronics*, vol. 28, no. 2, pp. 730–739, 2013.

27. S. Vazquez, J. Rodriguez, M. Rivera, L. G. Franquelo, and M. Norambuena, "Model predictive control for power converters and drives: Advances and trends," *IEEE Transactions on Industrial Electronics*, vol. 64, no. 2, pp. 935–947, 2017.